A Dynamic Model for Determining the Middle of *Escherichia coli*

Karsten Kruse
Max Planck Institut für Strömungsforschung, D-37073 Göttingen, Germany, and Institut Curie, Physicochimie, UMR CNRS/IC 168, 75248 Paris Cedex 05, France

ABSTRACT Proper placement of the division septum is an essential part of bacterial cell division. In *Escherichia coli*, this process depends crucially on the proteins MinC, MinD, and MinE. The detailed mechanism by which these proteins determine the correct position of the division plane is currently unknown, but observed pole-to-pole oscillations of the corresponding distributions are thought to be of functional importance. Here, a theoretical approach toward an explanation of this dynamical behavior is reported. Emphasizing generic properties of the protein dynamics, two features are found to be sufficient for generating oscillations: first, a tendency of membrane bound MinD to cluster; and second, attachment to and detachment from the cell wall, which depends on the amount of molecules already attached. The model is in qualitative agreement with the presently existing experimental results and further tests of the underlying model assumptions are suggested. Finally, based on the analysis of the model a simple mechanism is proposed on how these proteins might initiate septal growth. In addition, to ensure correct positioning of the septum, the MinCDE complex could therefore also play an important role in cell cycle control.

INTRODUCTION

Cytokinesis is the process by which a cell separates into two after its DNA has been duplicated and evenly distributed onto the two future daughter cells. For a successful division to take place the cell has to determine the location, where to separate, and the point of time to start cell cleavage. In *Escherichia coli*, as in other rod-like bacteria, separation into two daughter cells is achieved by forming a septum perpendicular to its long axis. In this process the septum grows inward, starting from the cell wall. The inner boundary of the growing septum is marked by a ring of FtsZ, a tubulin-like GTPase, that is thought to initiate and to guide septal growth by contraction (Lutkenhaus, 1993). Usually, the FtsZ-ring is positioned close to the center, but it may also form in the vicinity of the cell poles. This observation has led to the notion of potential division sites at which the contractile ring may be located (Teather et al., 1974; Donachie and Begg, 1996). A wild-type bacterium is supposed to contain three such sites located, respectively, at the center and close to the poles. They may be thought of as given by special proteins incorporated into the cell wall (Donachie and Begg, 1996).

Leaving the problem aside of how the potential division sites themselves are located at the correct positions, this notion immediately leads to the question by which mechanism the cell is able to make the right choice between them. Ample evidence has been collected that the products of the *minB* operon play a decisive role in this process. A first indication of this came from the observation that mutations in this gene locus may induce the formation of DNA-free cell fragments, so-called minicells (Adler et al., 1967; Davie et al., 1984). Later, deBoer et al. determined the products of this operon, namely MinC, MinD, and MinE (deBoer et al., 1989). In experiments modifying the expression of these proteins they showed that MinC is able to inhibit formation of the FtsZ-ring, while MinE may suppress this inhibition at any of the three potential division sites. Even though MinD, which is known to be an ATPase (de Boer et al., 1991) does not seem to interact directly with FtsZ, it is essential for proper septum placement because it is necessary for building a MinC-block at a division site and for suppressing such a block by MinE (deBoer et al., 1992).

Apparently, these proteins influence the position of the FtsZ-ring and hence of the division septum by interacting with the cell periphery. By fluorescent labeling, MinE was shown to attach to the cell wall only in the presence of MinD (Raskin and deBoer, 1997). The distribution of membrane-bound MinE is not uniform, but localized to a large extent in the central two-fifths of the cell, where it forms a pronounced ring. This ring is a structure independent of the FtsZ-ring, and starts to dissolve at the beginning of cytokinesis. On the contrary, MinD attaches to the cell wall even in the absence of MinE. In this case it is homogeneously distributed on the cytoplasmic membrane (Rowland et al., 2000). More interestingly, in the presence of MinE, the distribution of bound MinD changes periodically in time (Raskin and deBoer, 1999a): fluorescently labeled MinD can be observed to be located for $\sim$10–60 s in one half, then to dissociate from the membrane and to switch quickly to the other half. There it reassociates with the membrane and remains in that half for some time before it changes sides again, and so on. While MinD is bound in one half it moves along the cell wall and accumulates at the corresponding cell pole (Hu and Lutkenhaus, 1999; Hale et al., 2001).

The oscillations appear very early during the cell cycle and seem to persist even when the septum starts to grow. In

Submitted June 18, 2001, and accepted for publication October 23, 2001.

Address reprint requests to: Dr. Karsten Kruse, Max Planck Institut für Strömungsforschung, Bunsenstraße 10, D-37073 Göttingen, Germany. Tel.: 49-551-5176410; Fax: 49-551-5176409; E-mail: karsten.kruse@chaos.gwdg.de.

0006-3495/02/02/618/10 $2.00

constricting cells, however, the oscillatory pattern changes, as in each of the cell halves the distribution oscillates like in a nonconstricted cell (Hu and Lutkenhaus, 1999). If cell division is inhibited by repressing the expression of FtsZ, bacterial filaments form. In this case, too, the spatial period of the time-averaged MinD distribution doubles, after the cell has reached a certain length (Raskin and deBoer, 1999a). Since for cells modified in this way the oscillations persist, FtsZ is not necessary to generate the periodic relocations of MinD. The temporal frequency of the oscillations apparently depends on the ratio of MinD to MinE. If this ratio is increased by a factor of 5 to 10 from the wild-type value, then the frequency reduces by a factor of ~6 (Raskin and deBoer, 1999a). Furthermore, the dynamical behavior of MinD can be induced by N-terminal fragments of MinE (Rowland et al., 2000). In contrast to the full protein, though, the truncated forms of MinE fail to form a ring. Very recently it has been shown that the MinE distribution also oscillates and that the ring is not stationary (Hale et al., 2001). Finally, the distribution of MinC shows the same kind of oscillations as MinD (Hu and Lutkenhaus, 1999; Raskin and deBoer, 1999b), but it does not play an active role in this process. Indeed, MinD oscillates also in the absence of MinC, while MinC needs MinD to do so. The location of MinC is therefore thought to be directly imposed by MinD, e.g., through the formation of MinCD dimers.

The periodic relocation of MinD seems to be functionally linked to the determination of the cell's center: in the absence of these oscillations cell divisions occur in ~50% of the cases close to the cell poles, leading to minicells. The above observations suggest the following scenario of how *E. coli* determines its middle (Raskin and deBoer, 1999a): MinE induces oscillations in the distribution of MinD, such that on average most of MinD is located in the vicinity of the cell poles. With the position of MinC being determined by MinD, the same is true for the inhibitor. Hence, formation of the FtsZ-ring is preferentially blocked close to the poles and more likely occurs in the center.

In the following, a theoretical attempt is made to describe the dynamics of the MinCDE system to identify a possible mechanism underlying the oscillations. In particular, two possible implications of the experimental observations will be explored, showing that the oscillations might result from the interplay of rather simple physical processes. The first concerns the aggregation of membrane-bound MinD at the cell poles (Hu and Lutkenhaus, 1999; Hale et al., 2001). In the present work, this phenomenon will be attributed to attractive interactions between the MinD molecules themselves. The origin of the attractive interactions might, for example, be electrostatic forces due to charges present on the protein's surface. The second concerns observations of the mutual influence of MinD and MinE on their rates of association with and dissociation from the membrane. The dependence of the attachment rate of MinE on MinD is readily inferred from the findings that, in the absence of MinD, MinE molecules are found to be dispersed throughout the whole bacterium (Rowland et al., 2000), while they are localized at the cell periphery in the presence of the former (Raskin and deBoer, 1997). For MinD the opposite is true, as it is attached to the cell wall in the absence of MinE, but periodically detaches when this protein is present (Raskin and deBoer, 1999a).

A possible physical mechanism explaining the rates' dependence on the respective amounts of membrane-bound MinD and MinE is the following: let the ATPase MinD exist in two different conformations, depending on whether it is bound to ATP or not, and suppose that the ATP-bound conformation has a high affinity for the cell wall, whereas for the ATP-free conformation this affinity is low. If the rate of hydrolysis of MinD-bound ATP is small compared to the rate of association of MinD/ATP complexes to the membrane, then MinD will be found mostly at the cell periphery. A low affinity of MinE for the cell wall, but a high affinity for membrane-bound MinD would explain the influence of MinD on the attachment rate of MinE to the cell wall. If, finally, MinE bound to MinD increased the rate of ATP hydrolysis by this protein, then MinE would raise the dissociation rate of MinD from the cell wall.

Each of the proposed processes can be found in other contexts within biological cells. In vivo formation of aggregates of membrane-associated proteins has been reported in several cases. Notably, in *E. coli*, chemotactic receptors are found to cluster at one end of the bacterium (Maddock and Shapiro, 1993). The suggested ATP-dependence of the attachment rate of MinD and the MinE-stimulated ATP hydrolysis by this protein, are strongly reminiscent of some characteristics of myosin and actin, respectively. Indeed, myosin attaches to actin only in a specific configuration, which is linked to the binding of ATP, and if bound to actin, the rate of ATP hydrolysis by myosin is substantially increased (Hackney, 1996).

In the next section a mathematical description of these processes will be presented. The expressions used are chosen such that they capture the essential features of the observed phenomena, but neglect many details of the putative underlying mechanisms described above. This strategy of a "generic" model is suggested by the fact that detailed experimental data on these mechanisms are, for the time being, missing. The behavior of the model should therefore be of general relevance, i.e., independent of any specific mechanisms, as long as they lead to aggregation of membrane-bound MinD, a higher affinity for the cell wall of MinE induced by MinD, and an increase of MinD's detachment rate induced by MinE.

The main result will be that while each of the proposed processes alone only leads to stationary states, in combination they suffice to generate oscillations of the kind experimentally observed. In its simplest version, though, the model fails to reproduce the MinE-ring. As will be shown, this feature can be obtained without introducing any new

element into the model by only a slight modification of one of the expressions used. Furthermore, as will be explained in the Discussion, the MinE ring is not essential for correct septum placement by the MinCDE system. The Discussion also contains a comparison of model characteristics with experimental results, showing that the presented mechanism is a reasonable candidate for explaining the observed oscillations. Further possible tests of the underlying model assumptions are then suggested. Finally, it will be argued that the MinCDE system might play a role in the initiation of cytokinesis. These proteins could thus provide a subtle link between the spatial and the temporal regulation of cytokinesis in *E. coli*, supporting the view exposed in Shapiro and Losick (2000) that an understanding of bacterial processes requires knowledge of the bacteria's spatial structure.

THE MODEL

To introduce the model for the dynamics of the protein distributions, first the general setting will be described. Geometrically, the shape of *E. coli* is well-approximated by a cylinder and with respect to MinC, MinD, and MinE, the interior of the bacterium can reasonably be regarded as homogeneous. The possibly existing potential division sites have not yet been sufficiently functionally characterized, such that the cell wall, too, will in this context be considered as homogeneous. Consequently, the full system is invariant under rotations along its long axis. As indicated by experiments, the protein distributions, too, possess this symmetry (Raskin and deBoer, 1997), implying that a one-dimensional description is sufficient. Furthermore, because the reported temporal frequency of the oscillations is high compared to the cell's growth rate, the dynamics will be described in a system of constant length. Finally, boundary conditions are given by impermeable walls.

Within this frame, the distributions of MinD and MinE are described by the densities $d^{f,b}$ and $e^{f,b}$, respectively. Here, the superscripts distinguish between the densities of free molecules dissolved in the cytoplasm and of molecules bound to the inner membrane. The one-dimensional densities d^f and e^f are obtained from the three-dimensional distributions by projection onto the cell wall. The distribution of MinC will not be described explicitly because, as mentioned above, it follows the distribution of MinD. As for the dynamics, the motion of free molecules is taken to be purely diffusive, while the motion of membrane-bound MinD and the exchange of proteins between the cytoplasm and the cell wall are determined by the mechanisms sketched in the Introduction. In the following, it is shown how these mechanisms can be cast into simple formal expressions that capture their essential features.

Self-aggregation of bound MinD

Self-aggregation is a stochastic process of many interacting particles. This process is most easily described in the case of particles that are located on discrete distinguishable sites only. In addition to formal simplicity, a discrete set of possible positions would be biologically justified for MinD if this protein attached to the cell periphery by binding to membrane proteins. In the case that MinD may attach anywhere to the cell wall, each site represents a small part of this surface. Hence, consider a one-dimensional lattice of length L with neighboring sites separated by a distance Δ. The lattice thus consists of $N = L/\Delta$ sites that are labeled by the index i ranging from 0 for the leftmost up to $N - 1$ for the rightmost site. Each site may be occupied by at most one MinD molecule.

An isolated particle will diffuse on this lattice, i.e., within an interval of time Δt it will jump to one of the two neighboring sites with probability $D\Delta t/\Delta^2$, where $D > 0$ is the diffusion constant. Due to attractive intermolecular forces, this probability is increased for jumps toward other particles and decreased for jumps away from them. Within a cell, attractive forces between molecules are short-ranged. To keep the model simple, only particles on sites $i \pm 1$ and $i \pm 2$ are taken to modify the hopping probabilities of a particle located on site i. Explicitly, the probability to jump within an interval Δt from site i to site $i + 1$ is increased by an amount $p\Delta t/\Delta^2$, with $p \geq 0$ if a second particle is located on site $i + 2$. In contrast, it is decreased by an amount $\bar{p}\Delta t/\Delta^2$ with $D \geq \bar{p} \geq 0$ if a particle is present on site $i - 1$. For jumps from site i to site $i - 1$ the probabilities are accordingly modified.

In the case $p = 0$ and $\bar{p} = D$, this process strongly resembles the situation analyzed with models of diffusion-limited aggregation (Witten and Sander, 1983). There, a single particle diffuses until it touches an aggregate of particles and is immobilized, upon which a new diffusing particle is introduced into the system, and so on. In the following, for simplicity, only the case $\bar{p} = 0$ will be considered.

From this description of individual particles one passes to a description of the density of bound MinD by identifying the mean occupation number of site i with the density d^b_i at this site. In the mean-field approximation, the time evolution of this density is given by

$$\begin{aligned}\frac{d}{dt}d^b_i = &\frac{1}{\Delta^2}[D + p(1 - d^b_i)d^b_{i+1}]d^b_{i-1} \\ &+ \frac{1}{\Delta^2}[D + p(1 - d^b_i)d^b_{i-1}]d^b_{i+1} \\ &- \frac{1}{\Delta^2}[2D + pd^b_{i-2}(1 - d^b_{i-1}) + pd^b_{i+2}(1 - d^b_{i+1})]d^b_i.\end{aligned} \tag{1}$$

The first two terms describe occupation of site i by a particle formerly located at sites $i - 1$ and $i + 1$, respectively; the last term the opposite processes. To analyze the stability of the homogeneous state, it will be convenient to dispose of a continuous version of the above equation. By expanding d^b_{i+j} around $d^b_i \equiv d^b(x)$, one obtains $\partial_t d^b(x) = -\partial_x J_d(x)$ with

$$\begin{aligned}J_d = &-D\partial_x d^b + p\partial_x\left[(1 - d^b)d^{b^2} + \left(\frac{7}{6} - \frac{15}{12}d^b\right)d^b\partial_x^2 d^b\Delta^2\right. \\ &\left. - \left(\frac{5}{6} - \frac{1}{2}d^b\right)(\partial_d d^b)^2\Delta^2\right].\end{aligned} \tag{2}$$

Experiments in vitro have shown that MinE may form oligomers (Zhang et al., 1998). Therefore, one might be inclined to introduce an expression analogous to 1 or 2 also for this protein. Indeed, if instead of MinD, bound MinE is assumed to self-aggregate, oscillations can be generated. But in contrast to experimental findings, for the oscillations thus obtained MinD and MinE are almost half a period out of phase. In the presence of MinD self-aggregation, the essential properties of the model are not affected by an analogous current for bound MinE. Hence, it will not be considered further on.

Attachment and detachment dynamics

Consider an arbitrary isolated site on the cytoplasmic membrane to which a MinD molecule may bind. Provided this site is empty, the probability for such a binding event within a small interval of time Δt will be proportional to the number of free molecules present in the surroundings. Because each site is assumed to be occupied by at most one MinD molecule, no further binding will occur as long as a molecule is present. This leads to the probability of an attachment event in the interval Δt of $\omega_1(1 - d)d^f\,\Delta t$, where ω_1 is a constant and d equals one for a site occupied by a MinD

molecule and zero otherwise. The probability of detachment of an isolated MinD molecule is very small compared to the probability of attachment (Raskin and deBoer, 1999a) and is therefore set to zero in the model. As proposed above, the presence of a MinE molecule increases this probability considerably. Assuming that a site occupied by a MinD molecule may also accept a MinE molecule, the probability for such an event to occur in an interval Δt is written as $\omega_2 de\ \Delta t$, where ω_2 is a constant and e equals one for a site occupied by a MinE molecule, and zero otherwise.

With respect to MinE, the attachment rate is in the same spirit chosen to be $\omega_3 d(1 - e)e^{\mathrm{f}}\ \Delta t$, where ω_3 is a constant. That is, MinE attaches to the membrane only in the presence of membrane-bound MinD. Finally, the probability of a detachment event within Δt is assumed to be given by $\omega_4 e\ \Delta t$, with ω_4 = const. Identifying for MinD and MinE as previously the mean occupation number of a site on the membrane with the corresponding density of bound molecules, dynamic equations for these densities are readily written down (see Eqs. 3–6 below).

In the Appendix it is shown that without making reference to any specific microscopic mechanism, this attachment/detachment dynamics requires the consumption of ATP. In the present context, it thus provides the "motor" for the observed oscillations.

The dynamical equations

Because both processes, self-aggregation and protein exchange between the cell wall and the cytoplasm, involve MinD and occur at the same places, they are likely to mutually influence each other. Namely, the mobility of membrane bound MinD might depend on the presence of membrane bound MinE and the detachment rate of a MinD molecule on whether it is part of a cluster or isolated. In principle, strong effects are possible. For example, because detachment of MinD was argued to be associated with a conformational change of this protein, the detachment of one molecule might lead to the detachment of a whole cluster by inducing this conformational change on neighboring molecules (Changeux et al., 1967). However, in essence, the mechanisms of self-aggregation and attachment/detachment to the cell wall should persist as described. Also, experimental results on this point are lacking, such that no further element will be introduced into the model. Its dynamics is therefore specified by simply adding the various elements introduced above, i.e., by the following set of partial differential equations

$$\partial_t d^{\mathrm{f}} = -\omega_1(1 - d^{\mathrm{b}})d^{\mathrm{f}} + \omega_2 e^{\mathrm{b}} d^{\mathrm{b}} + D_{\mathrm{d}}\partial_x^2 d^{\mathrm{f}} \tag{3}$$

$$\partial_t d^{\mathrm{b}} = \omega_1(1 - d^{\mathrm{b}})d^{\mathrm{f}} - \omega_2 e^{\mathrm{b}} d^{\mathrm{b}} - \partial_x J_{\mathrm{d}} \tag{4}$$

$$\partial_t e^{\mathrm{f}} = -\omega_3 d^{\mathrm{b}}(1 - e^{\mathrm{b}})e^{\mathrm{f}} + \omega_4 e^{\mathrm{b}} + D_{\mathrm{e}}\partial_x^2 e^{\mathrm{f}} \tag{5}$$

$$\partial_t e^{\mathrm{b}} = \omega_3 d^{\mathrm{b}}(1 - e^{\mathrm{b}})e^{\mathrm{f}} - \omega_4 e^{\mathrm{b}}, \tag{6}$$

or its discrete analog. Here, D_{d} and D_{e} are the diffusion constants of cytoplasmic MinD and MinE, respectively. The equations do not contain source terms for either MinD or MinE, because it has been shown that the oscillations persist if their synthesis is blocked (Raskin and deBoer, 1999a).

To complete the definition of the model, the boundary conditions have to be specified. Because the system is contained between impermeable walls, for each density the current has to vanish at the boundaries. Consequently, a basis in the corresponding functional space is provided by $\cos(n\pi x/L)$, with n = 0, 1, 2,. . ., $x \in [0, L]$, and where L is the system length. For the discretized dynamics on a lattice, virtual sites are introduced at $i = -1$ and $i = N$ on which the density has the same value as on sites 0 and $N - 1$, respectively. Thereby, for all sites i = 1,. . ., $N - 1$ the aggregation dynamics of d_i^{b} is given by Eq. 1, and the homogeneous state is stationary.

RESULTS

To analyze the dynamical equations 3-6, first the case $e^{\mathrm{f}} = e^{\mathrm{b}} = 0$ will be considered, which allows studying the self-aggregation of membrane-bound MinD. Experimentally, this corresponds to the situation when the expression of MinE has been suppressed. Then the linear stability of the homogeneous state will be analyzed in the general case, revealing in particular the existence of oscillatory solutions. Finally, these oscillations will be investigated more closely by numerically integrating the discretized dynamics.

Self-aggregation of MinD

In the case $e^{\mathrm{f}} = e^{\mathrm{b}} = 0$, asymptotically, only Eq. 4 has to be considered. Thus, assume from the beginning $d^{\mathrm{f}} = 0$, implying that the dynamics is completely determined by the current J_{d}. The homogeneous state $d^{\mathrm{b}}(x) \equiv \bar{d}$ = const is stationary. By linearizing Eq. 4 with respect to this state, a perturbation of the form cos kx, with $k = n\pi/L$ and n = 0, 1,. . ., $N - 1$ is seen to evolve for short times t as $\exp\{\lambda(k)t\}$ cos kx, where

$$\lambda(k) = -(D + p(3\bar{d} - 2)\bar{d})k^2 + p\,\frac{\Delta^2}{12}\,(15\bar{d} - 14)k^4 \tag{7}$$

$$\equiv C_1 k^2 + C_2 k^4. \tag{8}$$

As long as $\lambda(k) < 0$ for all k, perturbations will thus decay and the homogeneous state is stable. A sufficient condition for stability is $\bar{d} > 2/3$, as it implies $C_1 < 0$. In contrast, if this inequality is invalidated and furthermore $p(2 - 3\bar{d})\bar{d} > D$, corresponding to a sufficiently strong attractive interaction between MinD molecules, then the system will evolve into an inhomogeneous stationary state. This state corresponds to one or several clusters formed by MinD.

Experimentally, such a distribution of membrane-bound MinD has not yet been reported. This might be simply due to the fact that in the experiments, the density of MinD satisfied the stability condition. Indeed, as will be seen below, for a given number of MinD molecules oscillations may exist in the presence of MinE, while the homogeneous distribution of membrane-bound MinD is stable in its absence. Therefore, a systematic study of the distribution of MinD as a function of the number of MinD molecules in the absence of MinE would be desirable.

Linear stability of the homogeneous state

In the general case, the homogeneous state $d^{\mathrm{f,b}}(x) \equiv \bar{d}^{\mathrm{f,b}}$ = const and $e^{\mathrm{f,b}}(x) \equiv \bar{e}^{\mathrm{f,b}}$ = const with

$$\bar{d}^{\mathrm{f}} = \frac{\omega_2 \bar{d}^{\mathrm{b}} \bar{e}^{\mathrm{b}}}{\omega_1(1 - \bar{d}^{\mathrm{b}})} \tag{9}$$

$$\bar{e}^{\mathrm{f}} = \frac{\omega_4 \bar{e}^{\mathrm{b}}}{\omega_3(1 - \bar{e}^{\mathrm{b}})\bar{d}^{\mathrm{b}}} \tag{10}$$

is a stationary state of the dynamics. If each of the four densities is expanded in the basis cos kx, the matrix corre-

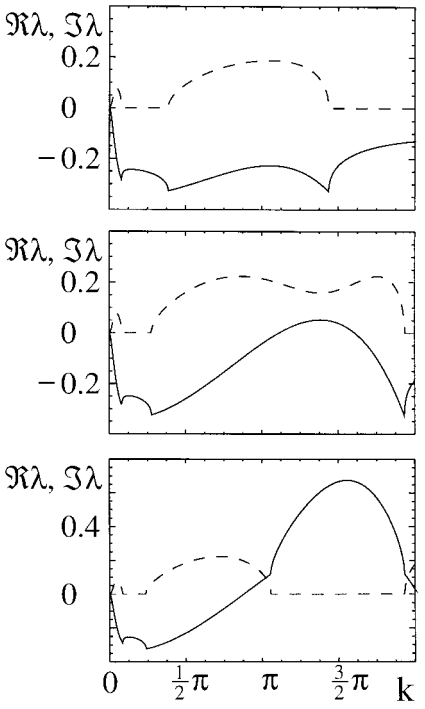

FIGURE 1 The eigenvalue λ with the largest real part of the linearized time evolution operator as a function of the continuous wave number k. Full lines represent the real part $\Re\lambda$, dashed lines the imaginary part $\Im\lambda$. The parameters are $\omega_1 = 1$, $\omega_2 = 10$, $\omega_3 = 1$, $\omega_4 = 0.1$, $D_d = D_e = 100$, $D = 3.25$, $L = 1$, $\Delta = 0.05$, $\bar{d}^b = 0.2$, and $\bar{e}^b = 0.05$. The parameter p takes the values 12 (*top*), 12.3 (*middle*), and 12.5 (*bottom*). In the middle case, the imaginary part is non-zero in the instability interval, indicating the existence of stable oscillatory solutions.

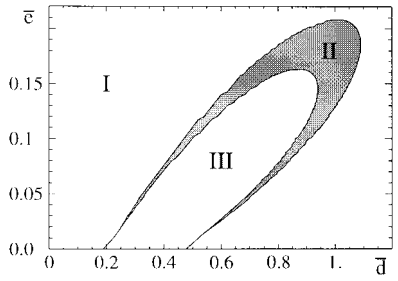

FIGURE 2 Phase-diagram as a function of the total molecule densities $\bar{d}$ and $\bar{e}$ resulting from the linear stability analysis. The remaining parameters are $\omega_1 = 1$, $\omega_2 = 10$, $\omega_3 = 1$, $\omega_4 = 0.1$, $D_d = D_e = 100$, $p = 12$, $D = 3.25$, $L = 1$, and $\Delta = 0.1$. In phase I the homogeneous state is stable, in phase II stable oscillatory solutions exist, and in phase III stationary nonhomogeneous states exist.

sponding to the linearized time-evolution operator is block-diagonal, with each 4×4 block belonging to a different wave number k. For each block k, let $\lambda(k)$ now denote the eigenvalue possessing the largest real part. Then, as in the previous section, $\lambda(k)$ determines the stability of the homogeneous state. Due to conservation of the number of molecules, again $\lambda(0) = 0$.

In the limit, when the exchange of molecules between the membrane and the cytoplasm is small compared to the aggregation dynamics of bound MinD, $\lambda(k)$ is approximately given by Eq. 7, with $\bar{d}$ replaced by $\bar{d}^b$. In this case, a separation of time scales leads to an effective decoupling of Eq. 4 from Eqs. 3, 5, and 6. An example is shown in Fig. 1, *bottom*, which presents the real and imaginary parts of λ as a function of the wave number k. In the absence of the self-aggregation current J_d, it is easy to show that $\lambda(k) \leq 0$ for all k. This remains true as long as aggregation is slow compared to the attachment-detachment dynamics (Fig. 1, *top*).

An example for the intermediate regime, where neither part of the dynamics dominates, is presented in Fig. 1, *middle*. As in the case discussed first, an interval of unstable modes exists. Remarkably, though, the imaginary part of $\lambda(k)$ is different from zero in this interval, implying the existence of oscillatory solutions. Formally, for the chosen parameter values, the homogeneous state loses its stability through a Hopf bifurcation as p is increased. Note that for small k, there is an interval of stable modes.

Numerical evaluation of $\lambda(k)$ reveals that the value of ω_2 has to exceed a critical value for oscillatory solutions to exist as p is increased. This reflects the necessity of a sufficiently strong interaction between MinD and MinE.

The parameters that may most easily be varied experimentally by genetically modifying *E. coli* are the numbers of MinD and MinE molecules. A typical example of a phase diagram based on the linear stability of the homogeneous state as a function of these two parameters is shown in Fig. 2. The region of instability of the homogeneous state extends in a rabbit's ear-like shape in the $(\bar{d}, \bar{e})$-plane, where $\bar{d} = \bar{d}^f + \bar{d}^b$ and $\bar{e} = \bar{e}^f + \bar{e}^b$. The ear consists of two parts: a core part, for which a stationary inhomogeneous attractor exists, and a boundary part, for which stable oscillatory solutions are present. For large values of the respective molecule densities, the homogeneous state is stable. This agrees with the experimental observation that overexpression of MinD or MinE suppresses the oscillations (Raskin and deBoer, 1999a). For low values, oscillations are also suppressed. As discussed above, depending on the amount of MinD, the system might then either evolve into the homogeneous state or into a stationary nonhomogeneous state. Note that the projection of the oscillatory phase on the $\bar{d}$-axis mostly falls into a region where the homogeneous state is stable. The instability ear shrinks when the value of Δ is decreased. This point will be further discussed in the next section.

Close to the point where the homogeneous state loses its stability, the dynamics is reasonably well-approximated by the linearized time-evolution operator. At this point, the corresponding solution is given by $d^b(x, t) = \bar{d}^b + D^b \cos(\Omega t + \phi_{d^b}) \cos(k_{cr} x)$, and analogously for the other densities. In this expression k_{cr} denotes the wave number of

the critical mode, which loses its stability first, i.e., $\Re\lambda(k_{cr}) = 0$ and $\Re\lambda(k) < 0$ for all $0 < k \neq k_{cr}$, where $\Re\lambda$ denotes the real part of λ. The oscillation frequency Ω is given by the imaginary part of $\lambda(k_{cr})$, and the coefficients in front of the cos and the phases are determined by the corresponding eigenvector of the linear operator. In the case $k_{cr} = \pi/L$ the solution of the linearized equations thus corresponds to a periodic relocation of the proteins from one cell pole to the other. For $k_{cr} > \pi/L$, the solution resembles the compartmentalized oscillations observed in bacterial filaments (Raskin and deBoer, 1999a). Because the model equations do not depend on the details of the proposed mechanisms, one finds that, generically, self-aggregation of MinD and mutual influence on the exchange of MinD and MinE between the cell wall and the cytoplasm generates oscillations resembling the ones observed in *E. coli*.

Averaged over time, the solution of the linearized dynamics at the bifurcation yields the homogeneous distribution. The mechanism for septum placement in the bacterium as described in the Introduction, however, depends crucially on an inhomogeneous average distribution of MinD. Therefore, the nonlinear regime will now be investigated.

Oscillations

The analysis of limit cycles, i.e., of oscillatory solutions of the model, is based on numerical integration of Eqs. 3-6. These solutions will be discussed only in terms of the densities d^b and e^b, because the densities of free molecules are much smaller and show only little time dependence. This is in agreement with the observation that the proteins are predominantly found at the cell periphery (Raskin and deBoer, 1999a; Hu and Lutkenhaus, 1999; Hale et al., 2001). In Fig. 3 the values of d^b and e^b at the boundaries are shown as a function of time for a solution obtained from a random initial condition. Clearly, this dependence is periodic, explicitly demonstrating the existence of oscillatory solutions. Maxima of the densities at one boundary coincide with minima at the other. This indicates transport from one end of the system to the opposite, and back. Concerning the growth period of d^b, two phases can be distinguished: a phase of slow growth and a subsequent phase of very fast growth during which the value gains about four-fifths of the oscillation amplitude. The decline toward the minimum is less abrupt, but still two phases of slower and faster change can be distinguished. This indicates quite sharp transitions between densities localized in either half of the system. For e^b these transitions are less pronounced. This density reaches its maximal value at a boundary shortly after the corresponding value of d^b has passed its maximum. The values of d^b and e^b are in phase, in the sense that they exceed the value of the corresponding homogeneous state in the same half of the temporal period. The extremal states for which the value of d^b at one or the other boundary is maximal are shown in Fig. 4. The corresponding densities

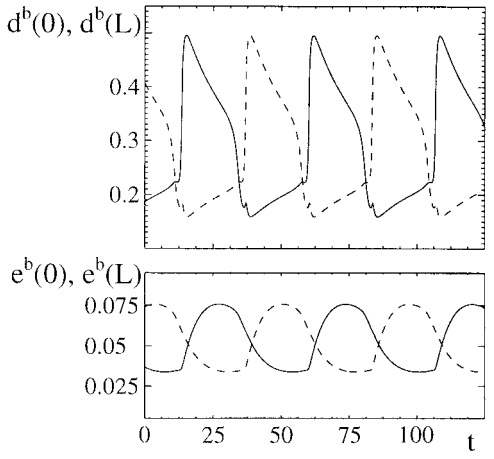

FIGURE 3 The boundary values of d^b (*top*) and e^b (*bottom*) as a function of time. Solid lines represent the values at the left boundary, dashed lines at the right boundary. The parameters are $\omega_1 = 1$, $\omega_2 = 10$, $\omega_3 = 1$, $\omega_4 = 0.1$, $D_d = D_e = 100$, $D = 3.25$, $p = 12$, $L = 1$, $\Delta = 0.05$, $\bar{d}^b = 0.2$, and $\bar{e}^b = 0.05$.

are localized close to one and the other boundary, respectively, such that the oscillations consist of transport from one end of the system to the other. Conclusively, these oscillatory solutions are qualitatively in agreement with the periodic relocations of MinD observed in Raskin and deBoer (1999a).

The time-average of the distributions are shown in Fig. 4. Contrary to the solution of the linearized system it is not homogeneous, but grows toward the boundaries. Furthermore, the averaged density is symmetric with respect to the system's center. For d^b one might distinguish a region of low average density in the central two quarters from a region of rather high density in the quarters adjacent to the boundaries. The time-average of d^b is approximately given

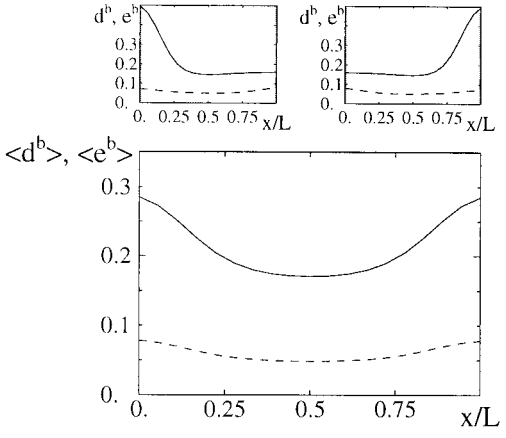

FIGURE 4 *Top*: The densities d^b and e^b at times when the respective boundary values of d^b are maximal. *Bottom*: Time-averaged distributions of d^b and e^b. Solid lines are for d^b, dashed lines for e^b. The parameters are as in Fig. 3.

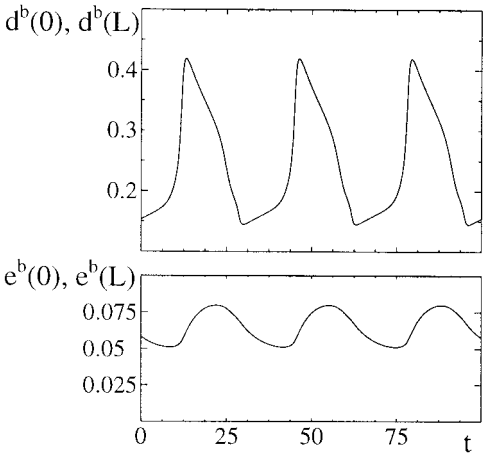

FIGURE 5 As in Fig. 3, but for $L = 1.5$. The functions for the right and the left boundary superpose.

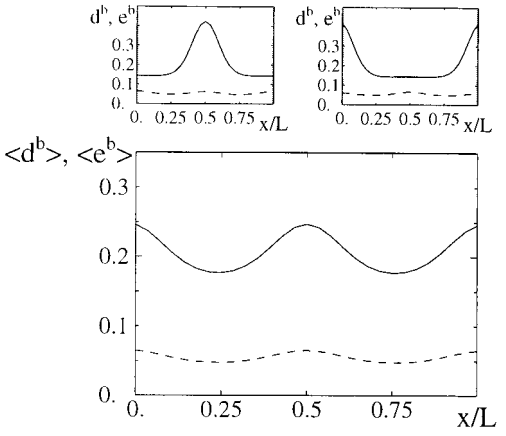

FIGURE 6 As in Fig. 4, but for $L = 1.5$.

by the average of the extremal distributions shown in the same figure, confirming the short transition times between them. These solutions therefore support the mechanism proposed in Raskin and deBoer (1999a) for septum placement in *E. coli* through an average depletion of MinD, and thus MinC in the bacteria's middle.

The mechanism leading to such a solution can be understood intuitively. To this end, it is helpful to divide the system in the center. Let d^b initially be located on the left. There, the current J_d will lead to a region of high d^b. In this region the attachment rate of e^b will become sufficiently large, such that e^b will also accumulate in the left half of the system. As it accumulates, d^b will start to decrease, ever faster as e^b increases, and relocate on the right. While d^b decreases, the attachment rate for e^b decreases, too, until there is eventually net detachment. Thereby the system is in a state that is mirror-symmetric with respect to the supposed initial state, and half a cycle is completed.

An oscillatory solution for a system 1.5 times larger, but all other parameters as before, is shown in Fig. 5. Again the boundary values of d^b and e^b are displayed as a function of time. The characteristics of these functions are very similar to the ones just described. In contrast to the previous example, the values for the left and right boundaries of the respective densities are now the same. The origin of this behavior is revealed in Fig. 6, where the densities for which the boundary values are extremal are displayed: the distributions now oscillate between two states, which are localized in the center and at the boundaries, respectively. The time-averaged distribution has therefore a spatial period of half the system size. Roughly, it can be thought of as being assembled from two solutions of the kind described previously that oscillate with a phase shift of half a temporal period. With respect to the previous example, the temporal period has increased by a factor of $\sim$1.5, comparable to the ratio of the two system sizes.

No simple relation has been found to exist between the oscillation frequency and the concentration of MinD and MinE or their ratio. Depending on the values of these concentrations, an increase of the ratio of MinD to MinE might result in an increase as well as in a decrease of the frequency. Therefore, the model is compatible with the observed reduction of the frequency as the MinD to MinE ratio is increased with respect to the wild-type value (Raskin and deBoer, 1999a). Nevertheless, further experiments are necessary to check whether this relation is general or, as the model suggests, depends on the expression level of MinD and MinE.

The solutions presented above are not the only type of oscillations in the system. A second class consists of localized densities d^b, for which the position of the maximum oscillates around the center with an amplitude of about a tenth of the system length. The changes in e^b are again comparably weak. All other oscillations observed can be thought of as assembled from the two basic classes described. Different oscillatory solutions may coexist. Furthermore, nonhomogeneous stationary states may coexist with oscillatory ones. Because they are similar to the time-averaged distributions presented above, they will not be further discussed. Numerical solutions for random initial conditions suggest that the number of coexisting limit-cycles increases with decreasing discretization length Δ. At the same time, the basins of attraction for solutions of the first kind seem to shrink. The origin of this behavior and the diminution of the instability ear mentioned above lies in the special form chosen to model the self-aggregation process. For reasons of simplicity, only the influence of neighbors had been taken into account. Therefore, as the discretization length Δ is decreased, the range of interaction between particles also decreases, and eventually vanishes. The dependence of the interaction range on the discretization length is, of course, nonphysical. For an interaction range independent of the discretization length these effects are

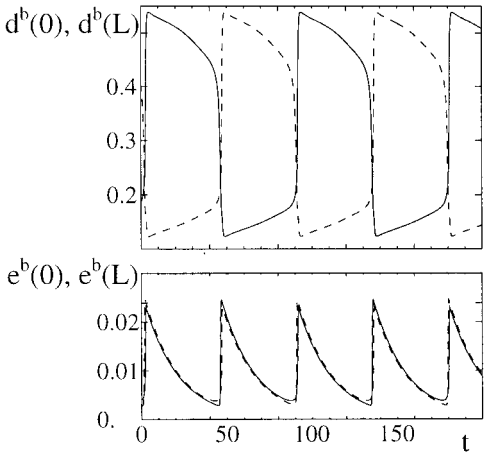

FIGURE 7 As in Fig. 3, but for the attachment rate of MinE given by expression 11. The parameters are $\omega_1 = 4$, $\omega_2 = 7$, $\omega_3 = 0.5$, $\omega_4 = 0.05$, $D_d = D_e = 10$, $D = 3.8$, $k_D = 4$, $L = 1$, $\Delta = 0.05$, $d_0^b = 0.2$, and $e_0^b = 0.03$.

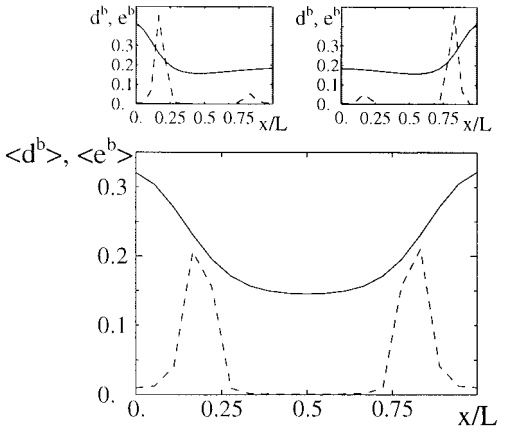

FIGURE 8 As in Fig. 4, but for the attachment rate of MinE given by expression 11. At the top the distributions are shown at a time for which e^b is maximally localized in one half.

likely to be suppressed, but further investigation is needed to clarify these points.

All numerically found limit cycles of the simple model 3-6 have in common that the density e^b is weakly structured and does not change a lot in the course of time. In contrast, experimentally, pronounced localization of MinE into a ring has been observed (Raskin and deBoer, 1997). Very recently, this structure has been reported to be highly dynamic (Hale et al., 2001). Since the MinE ring is such a prominent feature of the MinE distribution, the path of simplicity will now be left for a short trip into the domain of refined expressions. It will be shown that without introducing any principally new element into the model, oscillations can be obtained for which e^b localizes. This is done by using a special functional form for the attachment rate of e^b. Explicitly, $\omega_3 d^b$ will be replaced by

$$\omega_3 d^b \exp\left\{\frac{(d^b - d^b_{opt})^2}{\sigma}\right\}. \qquad (11)$$

This form reflects an optimal concentration of d^b for which e^b increases fastest. Fig. 7 shows an example of an oscillatory solution for this modified model. The time-dependence of the boundary values of d^b is now more rectangular-like, indicating this distribution to oscillate between two states. With respect to e^b, the functional form resembles a sawtooth, and the values at the two boundaries coincide more or less. Fig. 8 reveals, however, that the boundary values of e^b are not that interesting. Instead, in the time-averaged distribution, two pronounced maxima appear, reflecting a "ring" formation. On the top, d^b and e^b are shown at times for which the MinE distribution is maximally peaked on one side. As can be seen, except for a small peak on one side, the entire distribution is highly localized on the other.

DISCUSSION

In the preceeding sections a model for the dynamics of MinD and MinE in *E. coli* has been presented and analyzed. The processes on which the model was chosen to be built are derived from experimental observations and are known to play a role in other contexts in biological cells. It has been found that clustering of membrane-bound MinD in combination with attachment and detachment rates, which depend on the concentration of molecules present on the membrane, may generate oscillations in the MinD and MinE distributions. These oscillations consist of a periodic relocalization of MinD from one cell pole to the other, as has been observed for this protein in *E. coli* (Raskin and deBoer, 1999a). The key feature of this process, in the bacterium as well as in the model, is that the dwell time of the protein in either half is long compared to the time needed to change sides. Consequently, on average, MinD is present more at the cell poles than at the center. When the system length was increased, its ratio to the spatial period of the time-averaged distribution was observed to double. This is in agreement with observations on bacterial filaments (Raskin and deBoer, 1999a). While both MinD and MinE are essential to generate oscillations, for too large concentrations of these proteins the homogeneous state is stabilized. This corresponds to the observed suppression of the oscillations in the bacterium by over expression of either MinD or MinE (Raskin and deBoer, 1999a). These features of the oscillatory solutions make the model a reasonable candidate for explaining the basic mechanism underlying the pole-to-pole oscillations of MinD in *E. coli*.

Several tests of the model assumptions are possible. Self-aggregation of membrane-bound MinD should lead to stationary inhomogeneous distributions if the amount of MinD and MinE are appropriately chosen. In particular, in the absence of MinE, a systematic investigation of different

expression levels of MinD should provide evidence in favor of or against this process. The proposed mutual influence of MinD and MinE on their association with the cytoplasmic membrane seems to be a rather immediate consequence of the experimental observations made in Raskin and deBoer (1997, 1999a). Still, further characterization of this process is needed to reveal the underlying mechanism. Within the model the energy needed to maintain the oscillations was shown to be used during the attachment/detachment cycle of MinD and MinE. Blocking the hydrolysis of ATP by MinD should thus lead to a stationary distribution. If the mechanism proposed in the introduction is realized, then both MinD and MinE should in this case be attached to the cytoplasmic membrane. Of course, in vitro experiments studying self-aggregation of MinD and the association of MinD and MinE with the cytoplasmic membrane are highly desirable, but seem to demand a considerable experimental effort. A simpler way to test the model further is indicated by the roughly linear dependence of the oscillation period on the system length.

The expressions used to describe accumulation of membrane-bound MinD and the exchange of MinD and MinE between the cytoplasm and the cell wall are very simple. They were chosen to capture the essential properties of these processes. Although reproducing the key features of the MinDE system, the model can thus not be expected to contain all experimentally observed effects, let alone to be in quantitative agreement with the observations. One discrepancy is the absence of ring-formation of MinE. A slight modification of the expression describing the association of MinE with the cell wall showed, however, that such a structure can be generated within the present frame, without introducing any principally new element. Note furthermore that a modified MinE protein has been observed to be able to induce oscillations of MinD without itself accumulating into a ring (Rowland et al., 2000). A property of the model that has not been observed is the coexistence of qualitatively different oscillatory solutions. In fact, such a coexistence could be highly disadvantageous for the bacterium, as it might prevent correct septum placement. Because coexistence was found to be important only when the discretization length Δ was decreased, it is likely be a consequence of the special choice for the aggregation dynamics of membrane-bound MinD. More realistic expressions have to be tested to clarify this point.

The model supports the mechanism suggested in Raskin and deBoer (1999a) of septum placement in *E. coli*: in the oscillatory regime, the time-averaged distributions of MinD and therefore MinC are minimal in the center and increase toward the boundaries. Thereby, formation of the FtsZ ring is blocked preferentially close to the poles. For this kind of distribution an accumulation of MinE into a ring is not needed, as the analysis presented above shows. Following this idea, the minicell phenotype reported in Rowland et al. (2000) for truncated MinE has to have a different reason than the absence of the MinE ring. It could be simply due to the low temporal oscillation frequency that has been observed in this system: MinC is absent too long from one of the cell poles to effectively prevent septum formation at this position. Consequently, the basic mechanism underlying septum placement in *E. coli* might be very simple indeed. In present-day *E. coli* this mechanism has most probably been refined or supplemented by other mechanisms to increase fidelity. Still, in principle, proper septum placement could be achieved by a mechanism even more simple, namely by formation of an inhomogeneous stationary distribution. This in turn is feasible with only one type of protein and would thus consume fewer resources. Therefore, one might wonder, what are the oscillations really needed for?

Before the completion of cytokinesis, MinC, MinD, and MinE should be roughly equally distributed on the two future daughter cells. The results of the linear stability analysis indicate two possibilities of how this can be achieved without invoking an additional control mechanism. Obviously, the cell synthesizes these proteins at a rate comparable to the elongation rate of the cell, such that the ratio of the amount of MinD and MinE to the cell volume is constant. In the model, if the system length L is increased with all other parameters, in particular, $\bar{d}$ and $\bar{e}$, fixed, either the homogeneous state becomes stable again or the spatial period of the oscillations doubles. This is due to the interval of stable modes extending from $k = 0$ to some positive k (see Fig. 1, *middle*). In the bacterium, equipartition might thus be achieved either if the cell divides at a length for which the homogeneous state is stable or if period-doubling occurs before or at an initial stage of cytokinesis. A rehomogenization of the MinCDE distributions has up to now not been observed, but a piece of evidence for period-doubling has been reported in Hu and Lutkenhaus (1999). Therefore, the second possibility seems more likely. This might in turn require a coordination of the initiation of cytokinesis and period-doubling. A much more appealing possibility is, however, that *cytokinesis is induced by the period-doubling itself*. Compatible with the observed form of the oscillations, contraction of the FtsZ ring and thus cytokinesis might be initiated either through the absence of MinE or the presence of MinC or MinD in the vicinity of the FtsZ ring. The most likely candidate is certainly MinC, because it is already known to interact with FtsZ (maybe mediated by other proteins as, e.g., ZipA). In fact, if MinC induced contractions of FtsZ filaments, on one hand assembly of an FtsZ ring would be inhibited and on the other hand an existing ring would contract in the presence of MinC.

Initiation of cytokinesis in the above manner offers the possibility to model or even actually construct a cell with a very simple cell cycle. Imagine a cell whose genome is completely coded in plasmids and where copies of each plasmid are present in a fairly large number, such that they are homogeneously distributed within the cell. Assume furthermore that the plasmids are continuously replicated while

the cell grows. In such a setting division might be restricted to the most elementary task of cell cleavage, which in turn could be initiated by a mechanism very similar to the one sketched in the previous paragraph. In combination with a simple metabolism leading to cell growth, this might eventually lead to the identification of the necessary requirements for a minimally functional cell. It is very tempting to speculate on the relation of such a primitive cell with the first cells that have appeared in the course of evolution.

APPENDIX

Alternative representation of the attachment-detachment dynamics

For an isolated site on the cell wall, the attachment-detachment dynamics of MinD and MinE can be described by a four-state model. Here, the four states of the site correspond to 1) no molecule bound, 2) one MinD bound, 3) one MinD and one MinE bound, and 4) one MinE bound. If c_i denotes the average occupation of the state i, where $i = 1, 2, 3, 4$, then

$$\frac{d}{dt}c_1 = \omega_4 c_4 - \omega_1 \bar{d} c_1 \tag{A1}$$

$$\frac{d}{dt}c_2 = \omega_4 c_3 + \omega_1 \bar{d} c_1 - \omega_3 \bar{e} c_2 \tag{A2}$$

$$\frac{d}{dt}c_3 = \omega_3 \bar{e} c_2 + \omega_1 \bar{d} c_4 - (\omega_2 + \omega_4) c_3 \tag{A3}$$

$$\frac{d}{dt}c_4 = \omega_2 c_3 - (\omega_1 \bar{d} + \omega_4) c_4 \tag{A4}$$

Here, $\bar{d}$ and $\bar{e}$ denote the total number of MinD and MinE molecules, respectively. The constants ω_i specify the transition rates between the different states.

In the case $\omega_i \neq 0$, $i = 1, 2, 3, 4$, it can be easily shown that there is a unique attractor in the form of a stationary state. In this state, a nonvanishing current of magnitude $\omega_4 c_4$ exists. Therefore, it is a nonequilibrium structure and chemical energy is needed to maintain it.

I thank M. Bornens for telling me about MinD oscillations and M. Piel for making the reference Hale et al. (2001) available to me. I thank them, as well as S. Camalet, R. Fleischmann, F. Jülicher, and J. Prost for valuable discussions and helpful comments. This work was supported by the Max-Planck Gesellschaft through a Schlössmann fellowship. The kind hospitality of the Landau Institute for Theoretical Physics, Moscow, where part of this work was completed, is gratefully acknowledged.

REFERENCES

Adler, H. I., W. D. Fisher, A. Cohen, and A. A. Hardigree. 1967. Miniature *Escherichia coli* cells deficient in DNA. *Proc. Natl. Acad. Sci. U.S.A.* 57:321–326.

Changeux, J.-P., J. Thiéry, Y. Tung, and C. Kittel. 1967. On the cooperativity of biological membranes. *Proc. Natl. Acad. Sci. U.S.A.* 57: 335–341.

Davie, E., K. Syndor, and L. I. Rothfield. 1984. Genetic basis of minicell formation in *Escherichia coli. J. Bacteriol.* 158:1202–1203.

deBoer, P. A. J., R. E. Crossley, A. R. Hand, and L. I. Rothfield. 1991. The MinD protein is a membrane ATPase required for the correct placement of the *Escherichia coli* division site. *EMBO J.* 10:4371–4380.

deBoer, P. A. J., R. E. Crossley, and L. I. Rothfield. 1989. A division inhibitor and a topological specificity factor coded for by the minicell locus determine proper placement of the division septum in *Escherichia coli. Cell.* 56:641–649.

deBoer, P. A. J., R. E. Crossley, and L. I. Rothfield. 1992. Roles of MinC and MinD in the site-specific septation block mediated by the MinCDE system of *Escherichia coli. J. Bacteriol.* 174:63–70.

Donachie, W. D., and K. J. Begg. 1996. "Division potential" in *Escherichia coli. J. Bacteriol.* 178:5971–5976.

Hackney, D. D. 1996. The kinetic cycles of myosin, kinesin, and dynein. *Annu. Rev. Physiol.* 58:731–750.

Hale, C. A., H. Meinhardt, and P. A. J. deBoer. 2001. Dynamical localization cycle of the cell division regulator MinE in *Escherichia coli. EMBO J.* 20:1563–1572.

Hu, Z., and J. Lutkenhaus. 1999. Topological regulation of cell division in *Escherichia coli* involves rapid pole to pole oscillation of the division inhibitor MinC under the control of MinD and MinE. *Mol. Microbiol.* 34:82–90.

Lutkenhaus, J. 1993. FtsZ ring in bacterial cytokinesis. *Mol. Microbiol.* 9:403–409.

Maddock, J. R., and L. Shapiro. 1993. Polar location of the chemoreceptor complex in the *Escherichia coli* cell. *Science.* 259:1717–1723.

Raskin, D. M., and P. A. J. deBoer. 1997. The MinE ring: an FtsZ-independent cell structure required for selection of the correct division site in *Escherichia coli. Cell.* 91:685–694.

Raskin, D. M., and P. A. J. deBoer. 1999a. Rapid pole-to-pole oscillation of a protein required for directing division to the middle of *Escherichia coli. Proc. Natl. Acad. Sci. U.S.A.* 96:4971–4976.

Raskin, D. M., and P. A. J. deBoer. 1999b. MinDE-dependent pole-to-pole oscillation of division inhibitor MinC in *Escherichia coli. J. Bacteriol.* 181:6419–6424.

Rowland, S. L., X. Fu, M. A. Sayed, Y. Zhang, W. R. Cook, and L. I. Rothfield. 2000. Membrane redistribution of the *Escherichia coli* MinD protein induced by MinE. *J. Bacteriol.* 182:613–619.

Shapiro, L., and R. Losick. 2000. Dynamic spatial regulation in the bacterial cell. *Cell.* 100:89–98.

Teather, R. M., J. F. Collins, and W. D. Donachie. 1974. Quantal behavior of a diffusible factor which initiates septum formation at potential division sites in *Escherichia coli. J. Bacteriol.* 118:407–413.

Witten, T. A., and L. M. Sander. 1983. Diffusion-limited aggregation. *Phys. Rev. B.* 27:5686–5697.

Zhang, Y., S. Rowland, G. King, E. Braswell, and L. Rothfield. 1998. The relationship between hetero-oligomer formation and function of the topological specificity domain of the *Escherichia coli* MinE protein. *Mol. Microbiol.* 30:265–273.